Environmental Laboratory

US Army Corps of Engineers®
Engineer Research and
Development Center

Environmental Quality Technology Program

Multi-Sensor Systems Development for UXO Detection and Discrimination

Man-Portable Dual Magnetic/Electromagnetic Induction Sensor

David Wright, Hollis H. Bennett, Jr., Linda Peyman Dove,
John H. Ballard, Morris P. Fields, Tere A. Demoss,
and Dwain K. Butler

February 2008

Multi-Sensor Systems Development for UXO Detection and Discrimination

Man-Portable Dual Magnetic/Electromagnetic Induction Sensor

David Wright

AETC Incorporated
120 Quade Drive
Cary, NC 27513-7400

Hollis H. Bennett, Jr., Linda Peyman Dove, John H. Ballard, Morris P. Fields, and Tere A. Demoss

Environmental Laboratory
U.S. Army Engineer Research and Development Center
3909 Halls Ferry Road
Vicksburg, MS 39180-6199

Dwain K. Butler

Alion Science and Technology Corporation
U.S. Army Engineer Research and Development Center
3909 Halls Ferry Road
Vicksburg, MS 39180-6199

Final report

Abstract: An unexploded ordnance (UXO) survey instrument that simultaneously collects total field magnetic data and frequency domain electromagnetic (FDEM) data was developed and tested for the detection and characterization of buried UXO objects. The system comprised an FDEM sensor operating at a single frequency of 9.8 kHz and a cesium vapor magnetometer. The system was tested in dynamic survey (detection) and cued analysis (characterization) modes at the Naval Research Laboratory Blossom Point UXO test facility in Maryland and the U.S. Army Engineer Research and Development Center (ERDC) UXO test site in Mississippi.

During these tests, electromagnetic (EM)-induced bias in the magnetic data was mitigated by physically offsetting the magnetometer from the EM transmitter coils. In both detection surveys, the aggregate detection rate exceeded the detection rates for the individual component sensor technologies. The cued analysis tests performed at Blossom Point showed that features can be estimated using physics-based analyses. The location estimate errors provided by these analyses were consistently less than 0.3 m. The cued analysis data collected at the ERDC UXO test site have been used to provide position estimates for most of the emplaced targets at this site.

Contents

Figures and Tables

Figures

Tables

Preface

This report describes efforts undertaken as part of the Environmental Quality Technology (EQT) Program A (1.6.a), Unexploded Ordnance (UXO) Screening, Detection, and Discrimination Management Plan, UXO Detector Design Thrust Oversight (BA2/3) Major Thrust, UXO Technology Demonstration, Work Unit "UXO Hand-Held Sensor Design." The work documented in this report was performed from 1 September 2002 through 31 October 2003. Dr. M. John Cullinane, Technical Director for Military Environmental Engineering and Science, Environmental Laboratory (EL), U.S. Army Engineer Research and Development Center (ERDC), is the UXO Focus Area Manager for EQT. This project was funded through the EQT program previously cited.

John Ballard, ERDC, was program manager of the EQT Program A (1.6.a) UXO Screening, Detection, and Discrimination Management Plan during the execution of this project. Principal investigators for this work were Hollis "Jay" Bennett, EL, ERDC, and David Wright, AETC Inc.

This project was performed under the general supervision of Dr. David Tazik, Chief, Ecosystems Evaluation and Engineering Division, and Dr. Elizabeth C. Fleming, Director, EL.

COL Richard B. Jenkins was Commander and Executive Director of ERDC. Dr. James R. Houston was Director.

1 Introduction

Background

Electromagnetic induction (EMI) and total field magnetic (TFM) surveys are the two primary geophysical technologies used for unexploded ordnance (UXO) detection. Of these two technologies, handheld EMI sensors perform better against shallow UXO items, and can detect nonferrous submunitions. Cesium vapor magnetometers are effective against large, deep ordnance items that handheld EMI sensors cannot detect; however, they do not respond to nonferrous objects. For on-site visits requiring the use of both technologies, the cost of collecting these data sets is significantly reduced if they can be collected simultaneously in a single survey. In addition, simultaneous data acquisition provides accurate relative positioning of the two data sets. Coincident relative positioning, particularly in the vertical dimension, is a prerequisite for the successful application of advanced joint/cooperative inversion algorithms.

The technical barrier to simultaneous collection of EMI and total magnetic field data lies in the deleterious effect of the EMI transmitted field on the magnetic field measured by the cesium vapor magnetometers. These magnetometers track oscillations of the Earth's magnetic field occurring at frequencies <200 Hertz (Hz). For magnetic field oscillations >>200 Hz they simply measure the average effect of these oscillations. Typical operation of EMI devices produces large low frequency components of a time domain EMI field that attenuates the measured geomagnetic field. A frequency domain EMI system operating above 200 Hz should simply induce an offset in the measured magnetic data. The magnitude of this offset is a function of the strength and orientation of the transmitted EMI field relative to the Earth's geomagnetic field vector.

Approach and scope

A commercially available off-the-shelf (COTS) EMI sensor suitable for simultaneous deployment with cesium vapor magnetometers does not exist. As a result, a custom sensor, designated as model EM73, was developed by Geonics Ltd., Mississauga, Ontario, Canada, whereby the frequency of the transmit field in operation mode is 9.8 kilohertz (kHz) pushing it well past the 200 Hz threshold. In addition, a model G823A

cesium vapor magnetometer was procured from Geometrics, Inc., San Jose, CA.

After procurement of the EM73 sensor and a model G823A Cesium vapor magnetometer, a series of static tests were performed. These tests were designed to (1) characterize the EM73 sensor sensitivity and conformity with modeled responses to known test targets and (2) quantify the effect of the EM73 transmit field on the measured magnetic data.

Subsequent to the static tests and partially based upon the findings of these tests, the magnetometer was physically integrated with the EM73 sensor, and two separate field trials were performed. The first field trial was performed at the Blossom Point test facility in Maryland and was used primarily as a system shakedown test to verify sensor operation in both dynamic and cued investigation modes. Operational procedures for both modes were tested and finalized during this trial. A second field trial was performed at the ERDC UXO test site in Vicksburg, MS. The goal of this trial was to demonstrate and verify sensor operation in a benign topographic and geologic environment.

Chapter 2 of this report documents the approaches to multi-sensor integration. The design and hardware selected for the present multi-sensor system are described in Chapter 3. Static tests to characterize integrated system characteristics, fine tune the system design, and develop data processing/compensation procedures are detailed in Chapter 4. Chapter 5 describes the two field tests used to characterize the performance of the system under realistic field conditions. Finally, conclusions and recommendations for future system development are given in Chapter 6.

2 Multi-Sensor Systems Development Considerations

Background

The general consensus among researchers and practitioners is that multi-sensor datasets increase possibilities for successful application of advanced approaches for UXO discrimination and classification to reduce false alarms and associated unnecessary excavation costs. As discussed in Chapter 1, the geophysical methods most commonly used for UXO surveys are total field magnetometry (TFM) and electromagnetic induction (EMI). While both frequency-domain EMI (FDEM) and time-domain EMI (TDEM) systems are available for UXO applications, the TDEM systems are most commonly used for production surveys.

To obtain magnetic and EMI datasets over a UXO survey site, there are three basic options: (1) survey the site two times, once with each sensor; (2) survey the site once with a dual-sensor system; (3) survey the site once with a dual-mode single-sensor system. A major requirement for realizing the full potential of advanced approaches for discrimination/classification, such as cooperative and joint inversion, is that the two datasets be accurately co-registered (positioned relative to each other). While agreement is not total on the co-registration accuracy required, in general an accuracy of 2 cm or better is desirable. This desired accuracy is difficult to achieve for option 1 (i.e., two separate surveys over a site). For a dual-sensor system (option 2), with the two sensor types on a common platform (hand-held, man-portable, or towed), the desired co-registration accuracy is easily achieved. With option 3, where the same sensor is used to obtain the two types of data simultaneously, the data are exactly co-registered.

A practical constraint on acquisition of multiple datasets at a UXO cleanup site is cost. For option 1, geophysical data acquisition, processing and interpretation costs are essentially doubled compared to a single dataset baseline. With options 2 and 3, the geophysical data acquisition costs are essentially the same as the single dataset baseline, and processing and interpretation costs may be only marginally higher than for a single dataset.

Time, cost, and data quality considerations strongly favor surveys with hand-held, man-portable, and vehicular-towed *arrays* of sensors wherever possible. However, in heavily vegetated/wooded areas and in rugged terrain, surveys with hand-held or man-portable single sensor, dual-sensor, or dual-mode sensor systems are necessary.

EQT sensor requirements and feasibility workshop

An EQT workshop on the requirements for hand-held and man-portable sensor systems and feasibility and concepts of multi-sensor system development was held in May 2002 in Denver, CO. The workshop was attended by representatives of government agencies (Army, Navy, SERDP (Strategic Environmental Research and Development Program, USGS (U.S. Geological Survey)), universities, and private companies. A key component of the workshop was two brainstorming sessions directed to hand-held and man-portable sensor requirements and to feasible approaches to dual-sensor/dual-mode sensor systems.

Desired attributes of hand-held and man-portable sensor systems for UXO site surveys are:

- Integrated positioning capability
- Versatile deployment modes for rugged terrain and vegetated / wooded areas
- Compatible with surrounding "open area" surveys
- Capability for high-resolution data acquisition with commensurate depth of investigation for possible targets
- Digital data recording
  - With on-board data storage for requisite data volume or telemetry capability
  - For integrated geophysical and positioning data
  - For permanent / archival record
- On-board data analysis, processing and visualization
  - Quality control—to assure data quality and complete site coverage
  - Potential for "real-time" analysis capability
- Roles for single-sensor, dual-sensor, dual-mode sensor systems.

For an integrated dual-sensor system, consisting of a TFM and either an FDEM or TDEM sensor, the major problem is that the active EMI system transmitter will cause the TFM sensor to saturate (i.e., the transmitted EM field is much larger than the Earth's field and the dynamic range of the

magnetometer). Some of the possible approaches for integrating TFM and EMI sensors into a dual-sensor system include:

- Separation — the two systems are separated by sufficient distance to minimize interference/interaction
- Optimal placement — the magnetometer is placed in a null or minimum region of the transmitted electromagnetic (EM) field
- Bucking — a secondary EM transmitter generates a field that "cancels" the primary EM field to create a null/minimum region for placement of the magnetometer
- Timing/synchronization — magnetometer measurements are made during the off-time of a TDEM transmitter
- Compensation/correction — for response of magnetometer to FDEM transmitter frequencies (i.e., correct or compensate for magnetometer offsets)

EQT UXO Program Multi-Sensor Systems Development Thrust

The above considerations were major drivers for developing the EQT UXO Program. Investments of the Multi-Sensor Systems Development Thrust include (1) a man-portable dual-sensor system, (2) a hand-held dual-sensor system, (3) a towed-array dual-sensor system, and (4) a dual-mode sensor system that can be operated in hand-held single sensor or array, man-portable array, and vehicular towed array implementation. The thrust was directed to providing multi-sensor geophysical survey capability for all areas at a UXO cleanup site—large "open areas," rugged terrain, and heavily vegetated and wooded areas. This report documents the design and development of item 1. In the overall development thrust, all of the approaches listed above for integration of TFM and EMI sensors into a system were utilized in varying degrees. For the man-portable, dual-sensor system documented in this report, optimal placement, separation and compensation/correction were considered in integrating a TFM and an FDEM sensor.

3   Hardware

The system hardware is comprised of an EMI sensor, magnetometer, handheld data acquisition computer, integrated power supply, interconnection cables, and deployment hardware (backpack, mounting pole, wheels, etc.).

EM sensor

A preliminary version of the EM73 sensor was delivered in February 2003. After some initial testing, this unit was returned to the manufacturer (at their request) for additional modification (Figure 1). The final coil configuration of the EM73 uses three concentric coils: TX – transmit coil, RX – receiver coil, and BX – buckout coil. Figure 2 shows the active bucking configuration whereby the BX (compensating transmit coil) is used to negate the primary field at the RX – receiver coil. Secondary fields resulting from the presence of conductive material in the primary field will induce a response in the receiver coil. The inphase and quadrature components (relative to the primary field) of this EMI response vector are measured (in millivolts [mV]) and transmitted to the data acquisition computer via RS232 serial communication link. The EM sensor sample rate is nominally 10 Hz.

Magnetometer

The magnetometer selected for this project was a Geometrics model G823A. This sensor has the Larmor signal de-coupler and counter, mounted in the preamp electronics package. This configuration negates the requirement for an additional console, thus reducing the complexity of the survey deployment mechanics. This sensor provides total magnetic field readings (units are nano-Tesla (nT)) at a 10 Hz sample rate in ASCII format via a serial RS232 data connection.

Peripheral hardware

The EM73 development included modification of Geonics data logging software and hardware (supplied with the EM73) to provide for logging of the magnetometer data. The data logger is a Juniper Systems Allegro all-weather hand-held device outfitted with two serial ports (upgradeable to

six serial ports). Full documentation for the data logger is provided in the system manuals.

Figure 1. Dual EM/magnetometer sensor.
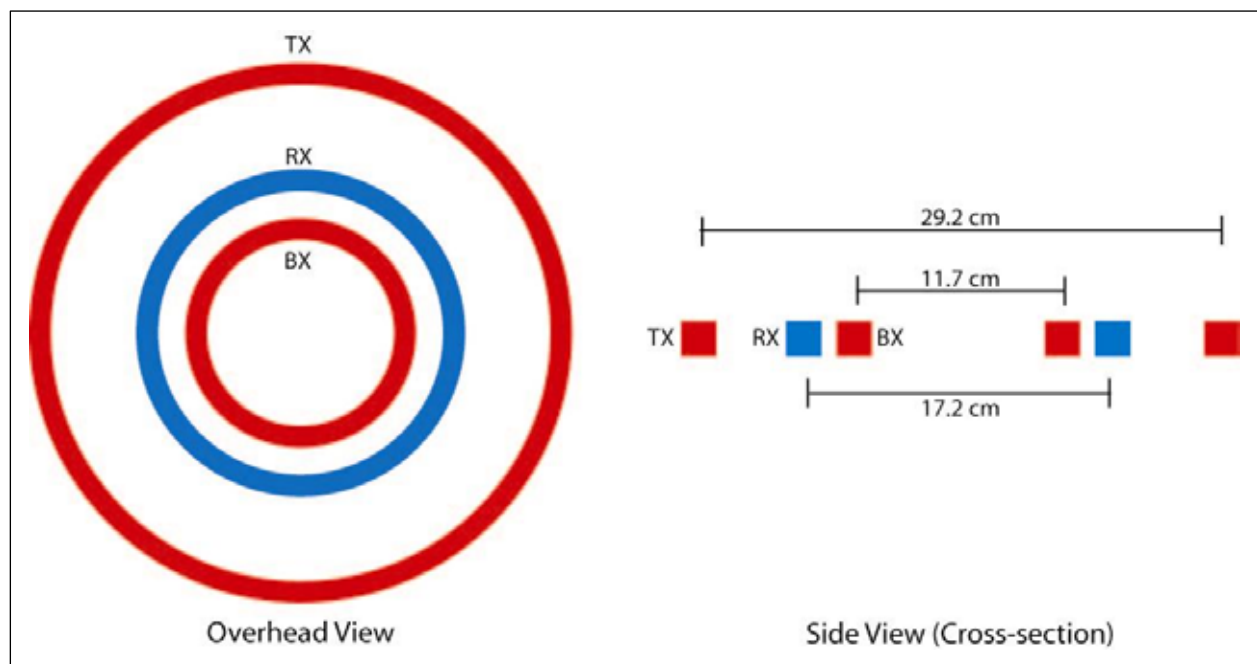
Figure 2. EM73 final coil configuration (TX - transmit coil, RX - receiver coil, BX – buckout coil).

A "gel-cell" lead acid 12-volt direct current [12-V(DC)] battery with a 12 amphere per hour (amp/hr) capacity was supplied as part of the EM73 sensor development. This capacity is sufficient to operate the EM73 for 40 hr between charging. In an effort to simplify and reduce the weight of the deployment hardware, a Vicor 12-V(DC) to 24-V(DC) converter was installed to provide the required power source for the magnetometer sensor using the same battery. Although this reduces the run time available between charging to 4 hr, it is preferable to change batteries between data collections rather than carry the weight of a second battery pack dedicated to the magnetometer. In addition, if a second battery pack were used, it would most likely require changing between data collections anyway.

Mechanical and electrical integration of the magnetometer with the EM73 sensor consisted primarily of (1) additional power and signal cables for the magnetometer and (2) geometric arrangement (positioning) of the two sensors based upon the results of static tests performed during the development (see Chapter 4).

4 Static Tests

Static tests were performed to characterize the sensitivity of the EM73 sensor, verify the EM73 model parameters with respect to coil configuration, dipole moment, and receiver gains, and characterize the effect of the EM transmit field on the magnetometer data.

Sensitivity tests

The EM73 development entailed trying a number of coil configurations. Of these, two configurations were delivered for evaluation. Sensitivity tests were performed on both versions of the EM73 as well as a GEM3 sensor (manufactured by Geophex Ltd., Raleigh, NC) to provide a comparison of sensor sensitivities. Two steel spheres (4- and 1-in. diameters) were measured at varying distances directly below the instrument coil centers. Figures 3 and 4 show that the EM73 appears to have signal-to-noise (S/N) characteristics comparable to those of the GEM3 for the 4-in.-diameter sphere and superior S/N for the 1-in.-diameter sphere. In both cases an improvement in S/N can be seen with the final EM73 (version 2) relative to the original EM73 (version 1).
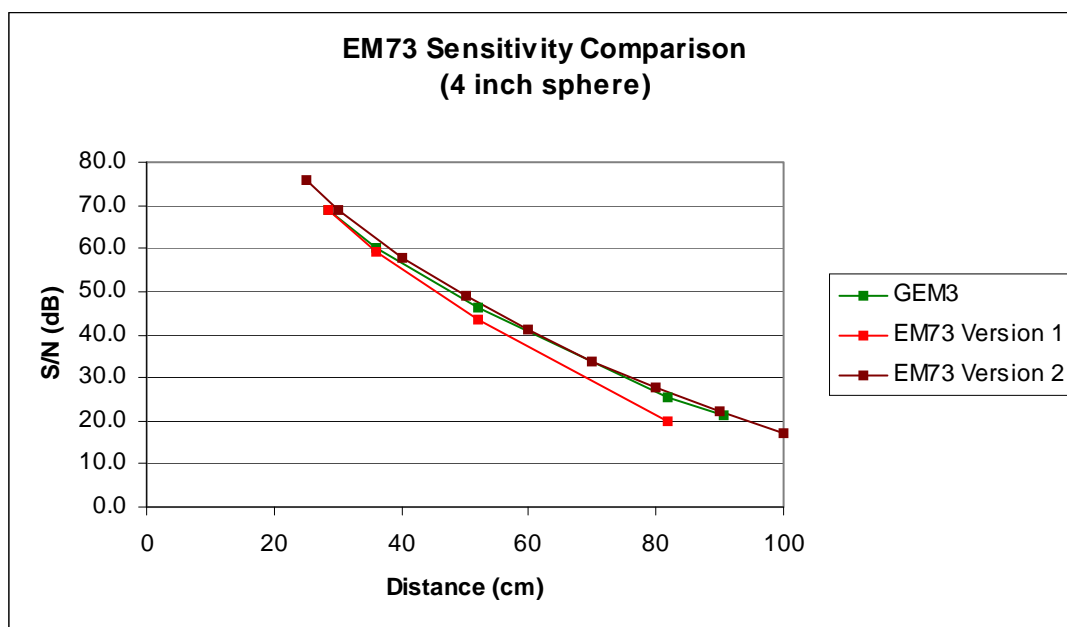
Figure 3. Sensor sensitivity test results for a 4-in.-diameter sphere placed at varying distances along the centerline of the coil axis. S/N decibels (dB) calculated as 20 x log (signal/noise).
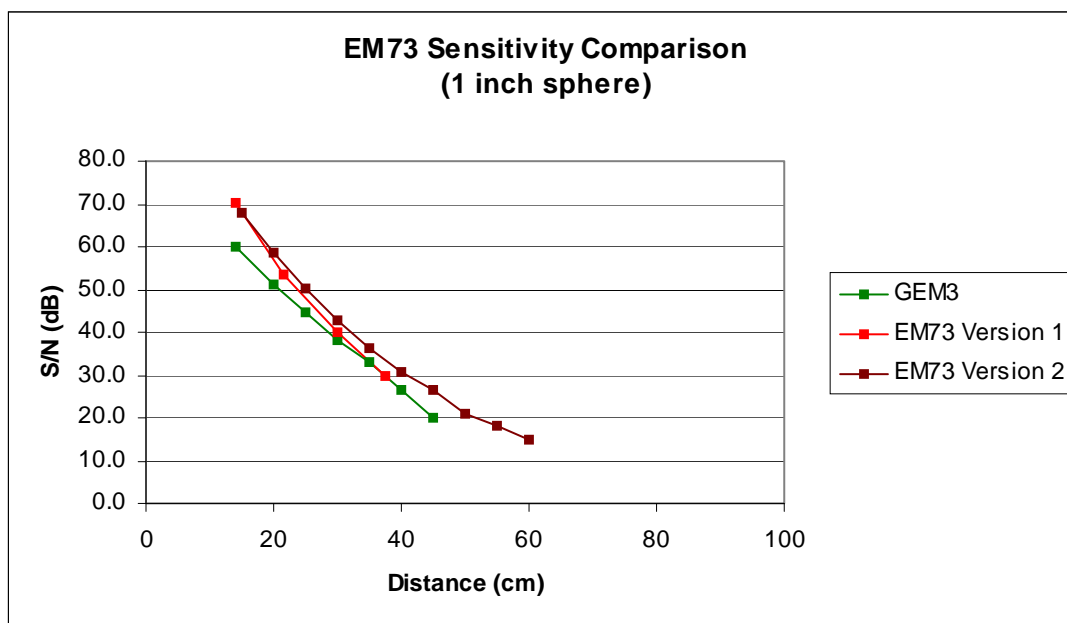
Figure 4. Sensor sensitivity test results for a 1-in.-diameter sphere placed at varying distances along the centerline of the coil axis. S/N (dB) calculated as 20 x log (signal/noise).

EMI sensor characterization tests

Analysis of spatially distributed EMI response data collected over a target may be used to estimate features relating to this target such as location, depth, size, and (limited) shape information (Khadr et al. 1998; Bell and Barrow 2000). In turn, these estimates may be used to guide remediation efforts by providing accurate location and a means of prioritizing a proposed dig list program. Briefly described, these analyses are performed by iteratively determining the dipole model that best fits the observed data. This model is parameterized by its position relative to the sensor, orientation, and three orthogonal polarizability tensors that are commonly referred to as "betas". The betas are used to infer the target size, aspect ratio, and axial symmetry.

A prerequisite for these analyses is that the EM sensor characteristics are known, including frequency, coil dimensions, transmit moment, receiver area, and gain settings. These characteristics, listed below, were provided by Geonics. Later in the program, the main and compensation transmitter dipole, and net moments were refined based upon empirical data obtained from test stand and bench measurements.

EM73 Coil characteristics provided by Geonics:

> *TX – transmit coil:*
> *mean diameter = 29.2 cm*
> *dipole moment = 3.65 Am² $_{p-p}$ = 1.29 Am² $_{rms}$*
>
> *BX – buckout coil (compensation transmit coil):*
> *mean diameter = 11.7 cm*
> *dipole moment = 0.75 Am² $_{p-p}$ = 0.27 Am² $_{rms}$*
>
> *Net Tx moment = 2.9 Am² $_{p-p}$ = 1.02 Am² $_{rms}$*
>
> *RX – receiver coil:*
> *mean diameter = 17.2 cm*
> *area   = 4.64 m²*
>
> *Receiver gain = 250 without Rx coil, 1,160[m²] with Rx coil*

Experimentally determined EM73 transmit coil moments:

> *TX – transmit coil:*
> *dipole moment = 3.28 Am² $_{p-p}$ = 1.16 Am² $_{rms}$*
>
> *BX – buckout coil (compensation transmit coil):*
> *dipole moment = 0.59 Am² $_{p-p}$ = 0.21 Am² $_{rms}$*
>
> *Net transmit coil = 2.68 Am² $_{p-p}$ = 0.95 Am² $_{rms}$*

The combined EM/magnetometer sensor was used to collect static measurements of a set of spheres, cylinders, and selected inert ordnance to verify the characterization of the system response (Figure 5). During these tests, the sensors were mounted in a fixed position and operated simultaneously. The targets were then sequentially placed at each node of a fixed 7-pt × 7-pt grid located directly beneath the sensors. For each placement, sensor data were recorded for a 5-sec period (nominal). The spacing between each grid node was 15 cm. Background readings were taken at the start and end of each series of 49 measurements to allow for removal of EM sensor drift and magnetic diurnal variations.
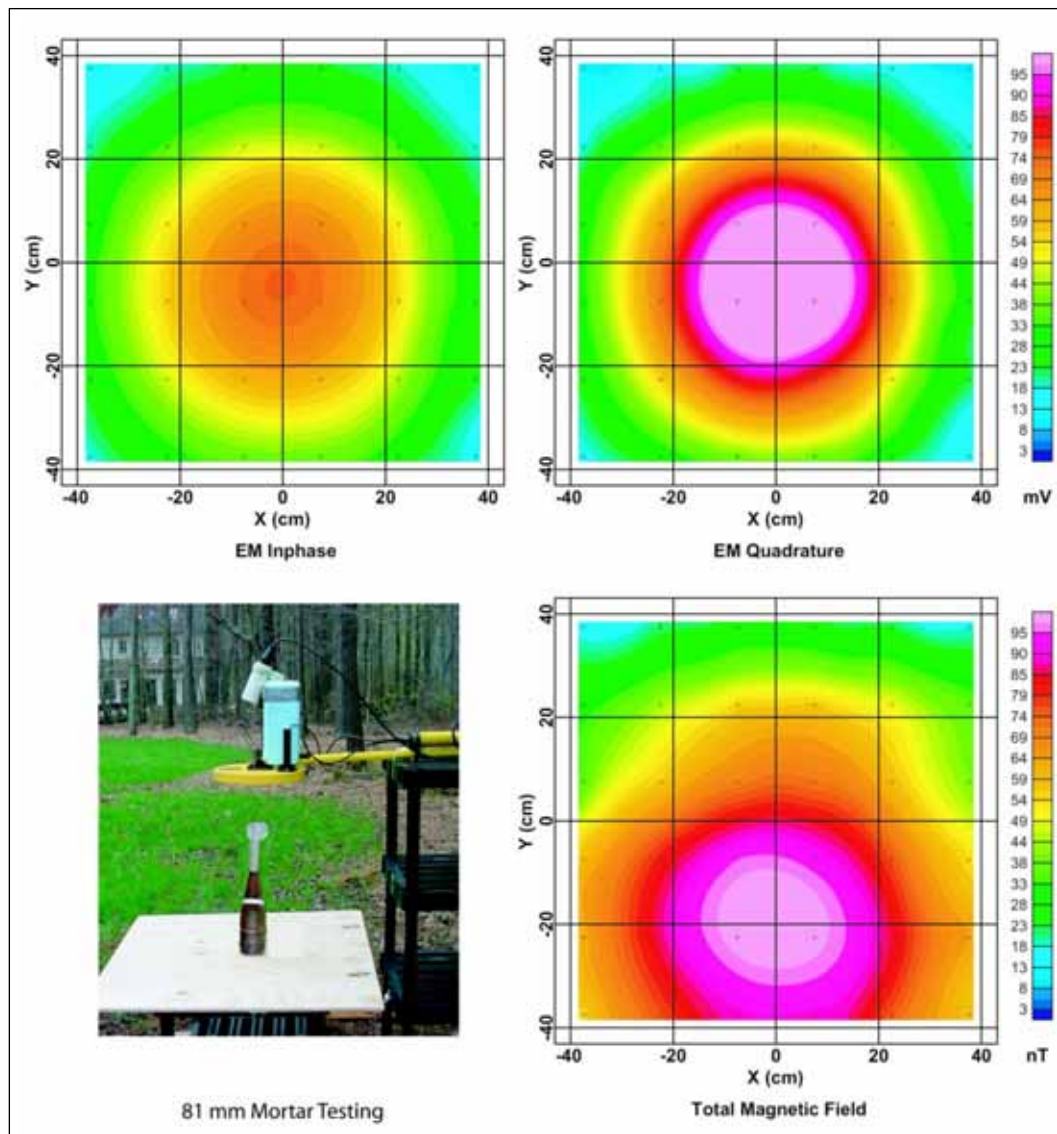
Figure 5. Simultaneously collected test stand data for an 81 mm mortar. The upper panels present the EM inphase (left) and quadrature (right) component responses in millivolts. The lower left panel shows the test set-up, and the magnetometer data (nT) are presented in the lower right panel.

Dipole-fit analyses were separately performed on the magnetic data (as described in Nelson et al. 1998a) and each component of the EM data. Successful recovery of target features (e.g., depth below sensor) was achieved; however, the EM quadrature component provided a better fit of the modeled dipole with the observed data than the inphase component of the EM or the magnetic data. Fitting of the inphase data does not perform as well due primarily to residual errors arising from nonlinear drift. Similarly, some of the magnetic fit results show a slight mis-coregistration due

to the presence of uncorrected magnetic signals from cultural sources. Figure 6 shows the successful dipole fit results for a steel rod.

4" by 0.5" steel rod, horizontal, parallel to Y axis.
Solid lines = data, Dashed lines = dipole model fits

| 043014B Total Field | 043014B EM73 In Phase | 043014B EM73 Quadrature |

Fit coherence = 0.991
Fit depth = 46.7 cm
Dist center of target to center of mag housing = 48.0 cm

Fit coherence = 0.999
Fit depth = 24.8 cm
Dist center of target to bottom of coil housing = 23.0 cm

Fit coherence = 0.999
Fit depth = 24.8 cm
Dist center of target to bottom of coil housing = 23.0 cm

Figure 6. Example of dipole fit analysis results.

EM sensor drift

All frequency domain EM sensors are susceptible to baseline (zero level) drift resulting from temperature-induced changes in the transmitter, receiver, and nulling coil properties. Two potential problems arise from this type of drift. The first problem is that, if the drift is severe enough, the instrument may run out of dynamic range. The EM73 sensor has a dynamic range of +/- 2047 mV. Nulling controls are provided so that the EM signal may be centered at 0 mV to compensate for gross drift effects that will occur under various ambient temperature conditions. Under most conditions, after a sufficient instrument warm-up period, this nulling of the sensor allows the user to remove the majority of the drift and operate the sensor successfully within the 4094 mV absolute dynamic range. During the static tests, however, drift was observed that exceeded the dynamic range of these nulling controls. This sensor limitation was addressed prior to the field tests by expanding the nulling control range of EM73, thus allowing operation in a broader range of ambient environmental temperatures. This modification did not change the calibration of the system, or the measurement dynamic range of the system.

Even after proper warm-up and nulling of the sensor, the system still exhibits some drift. One method of removing this drift is to take "background" readings at the start and end of each set of measurements and remove the interpolated (based on time) values between these readings from the measured data. This process, known as "background leveling," is used primarily during cued analyses or static test measurements and assumes that the drift is linear between background readings. If the drift is nonlinear, the time between background readings must be shortened until the assumption of linearity is valid. A second method of drift removal is the application of a response frequency-based filter. This method is suitable for dynamic survey data acquisition because the target response periodicity is significantly different than what would be expected of instrument drift. In practice, simple de-median filters are used to remove this drift as well as geologic signal from survey data. Figure 7 presents an extreme example of the EM sensor drift and the results from using both methodologies to level the data. The nonlinearity in the drift is presumed to be due to variable sunlight conditions during data acquisition. The background measurement intervals correspond to those used during static testing. For future static testing, a sunlight shield and/or shorter intervals between background measurements will serve to mitigate the effects of this drift. The de-median filter is appropriate for detection of UXO and is commonly used to remove geologic signal as well as any other long wavelength response from survey data.

EM-induced heading errors

The EM signal imposes a bias (offset), in the magnetometer data. This bias is a function of the strength of the EM field and its orientation with the Earth's magnetic field. Figure 8 shows the offset in the magnetic response over a horizontal plane 0.25 m above the EM sensor. With each grid node positioned beneath the magnetometer sensor, the EM sensor was cycled on and off. The offset observed when the EM was active is assumed to be the induced heading error. Clearly changing the orientation of the magnetometer and EM sensors with respect to the Earth's magnetic field will induce changes in the magnetometer reading. These errors are not a problem for static testing or cued analysis during which the sensor orientation can be reasonably controlled. Under dynamic survey conditions, the magnetometer must either be positioned greater than 0.5 m from the center of the EM coil, or these errors must be compensated for by using an independent measure of the sensor orientation in the Earth's magnetic field. Implementation of the latter was beyond the scope of this development;
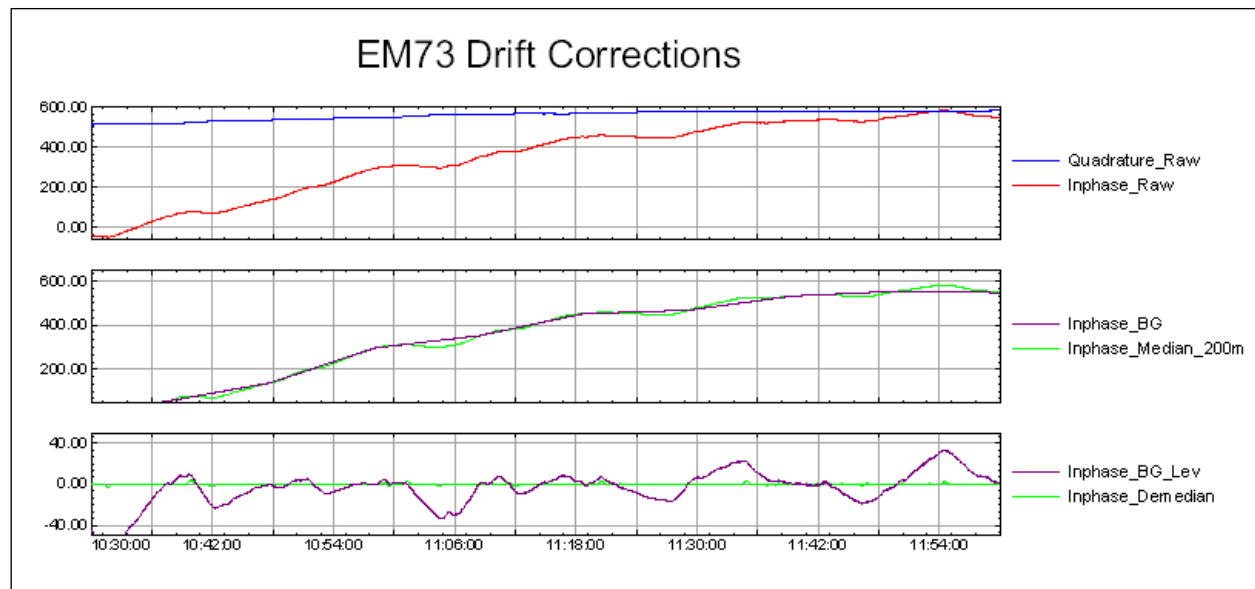
Figure 7. Example of EM sensor drift and leveling results (shown for in-phase only) using both background removal (purple) and de-median filter (green). Vertical scales are sensor response (millivolts) and the horizontal scale is time (hh:mm:sec).
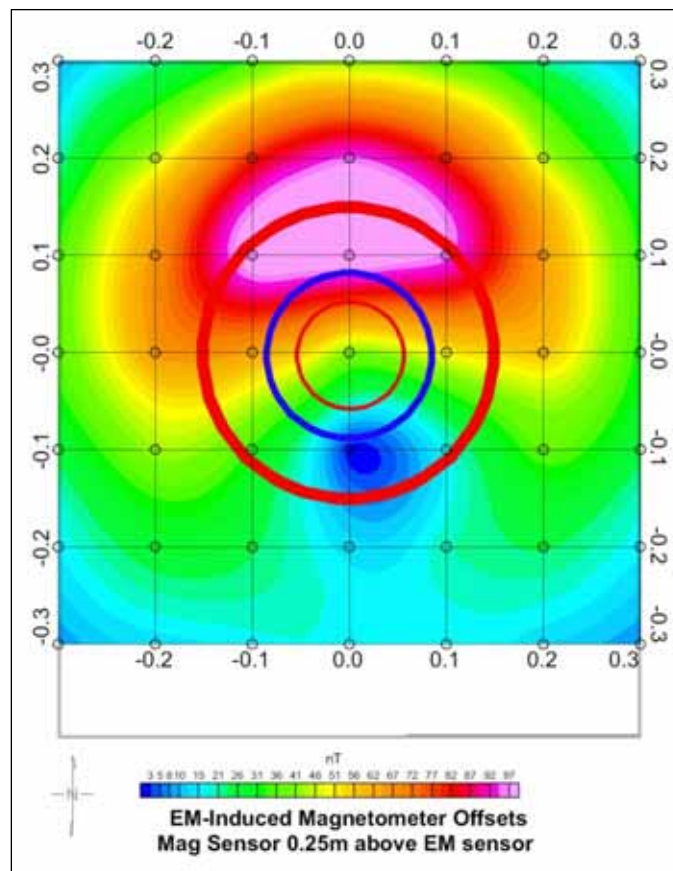
Figure 8. Color grid representation of EM-induced bias in the measured magnetic data.

therefore, deployment of this prototype during field trials relied upon the former approach. It bears mention that previously discussed geology removal filters will also remove these heading errors provided their periodicity is sufficiently separate from that of our intended targets.

Although the implementation of a compensation methodology was beyond the scope of the current project, additional efforts to confirm our understanding of the problem and show the viability of a compensation based solution were performed. The EM sensor causes the Earth's magnetic field to oscillate at 9.8 kHz. The magnetometer measures the magnitude of the Earth's magnetic field vector. This magnetic field vector is the vector sum of the Earth's static field and the oscillating EM field. For fields oscillating at greater than 200 Hz, the magnetometer measures the average effect of these fields (confirmed by Kenneth Smith of Geometrics Ltd). The average effect of that component of an EM field that is aligned with the Earth's magnetic field will be zero; however, the component of the EM field that is normal to the Earth's field will always result in an increase in the magnitude of the measured total field. The magnitude of the Earth's magnetic field vector in the presence of an oscillating EM field can be expressed as:

$$H_{meas}^2 = <H_{earth}^2 + H_{orth\_EM}^2>$$

Where $< >$ denotes time averaging and H_{orth_EM} represents the component of the time varying EM field that is orthogonal to the Earth's magnetic field vector.

Under the assumption $H_{earth} >> H_{orth\_EM}$, the resulting effect of the EM field can be expressed (i.e., the EM-induced heading error) as:

$$Herr = \tfrac{1}{2} < Horth\_EM2> \div Hearth$$

Figure 9 shows the observed heading errors on the left juxtaposed with the modeled EM-induced heading errors in the center and the residual errors (after subtracting the modeled errors from the observed errors) on the right. The modeled data were based on a coarse estimate of the total magnetic field vector components (derived from the geographic position of the transmit driver interface connection and the IGRF2000 geomagnetic field model). These results indicate that, given a measure of our combined sensor attitude with respect to the Earth's magnetic field, it is possible to compensate the EM-induced heading errors.
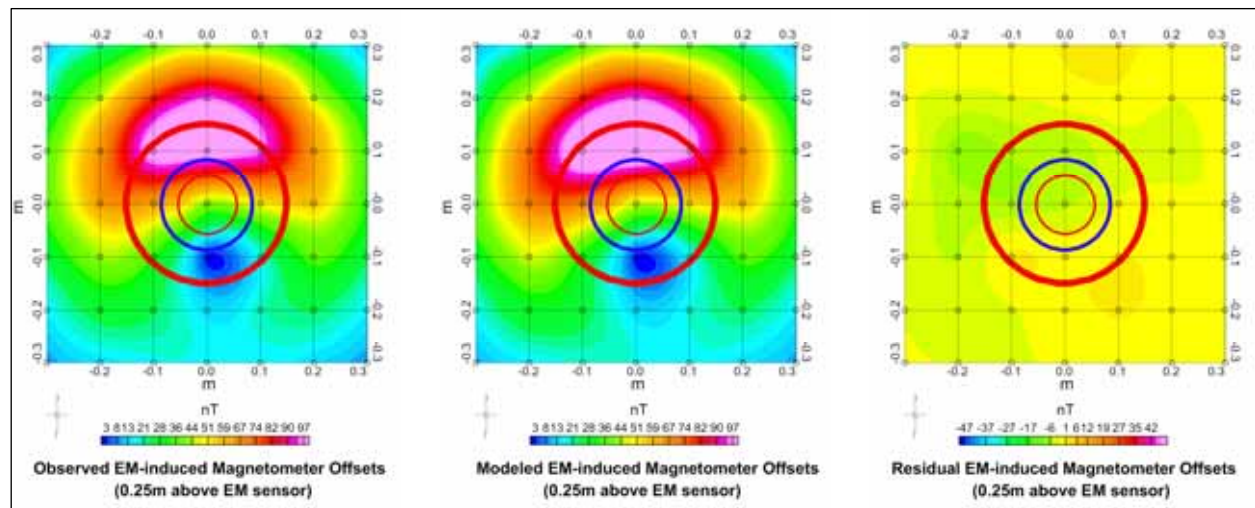
Figure 9. Observed, modeled, and residual EM-induced errors in the measured magnetic data. The EM transmit coil positions are shown in red. The asymmetry in the residual error plot occurs near the physical location of the transmit driver interface connection.

5   Field Tests

The final phase of this development project involved performing two field trials of the system. The first trial was performed at the Naval Research Laboratory's (NRL's) Blossom Point test facility near La Plata, MD. The objective of this trial was to test and finalize the sensor deployment procedures in both a dynamic survey mode for ordnance detection and a cued analysis mode for ordnance discrimination.

The second trial was performed at the U.S. Army Engineer Research and Development Center's (ERDC's) UXO test site in Vicksburg, MS. The objective of this trial was to demonstrate the system operation to ERDC personnel, incorporating the lessons learned from the first trial.

Field Test 1: Blossom Point, MD

Dynamic survey test description

This trial was performed 25–28 August 2003. A dynamic survey for UXO detection was performed over the NRL UXO test field. This field is approximately 100 m x 30 m and is seeded with various UXO and clutter targets (Nelson et al. 1998b). The field is relatively flat and grass covered. The dual sensor system was deployed in a man-portable wheeled configuration with the magnetometer offset behind the center of the EM sensor by 0.5 m relative to the direction of travel.

Sensor navigation was performed using strings stretched across the ground parallel to the intended survey line direction. These strings were spaced at 2-m intervals, and the sensor line spacing was 0.33 m. Cross-track sensor positions were assumed to be along the intended survey line. Down-track positions were determined by interpolating between manual fiducial marks taken as the EM coil head crossed the survey boundaries at the start and end of each line.

Dynamic survey findings

The survey data were positioned and presented in color grid format for review as shown in Figure 10. Visual inspection of these data shows the
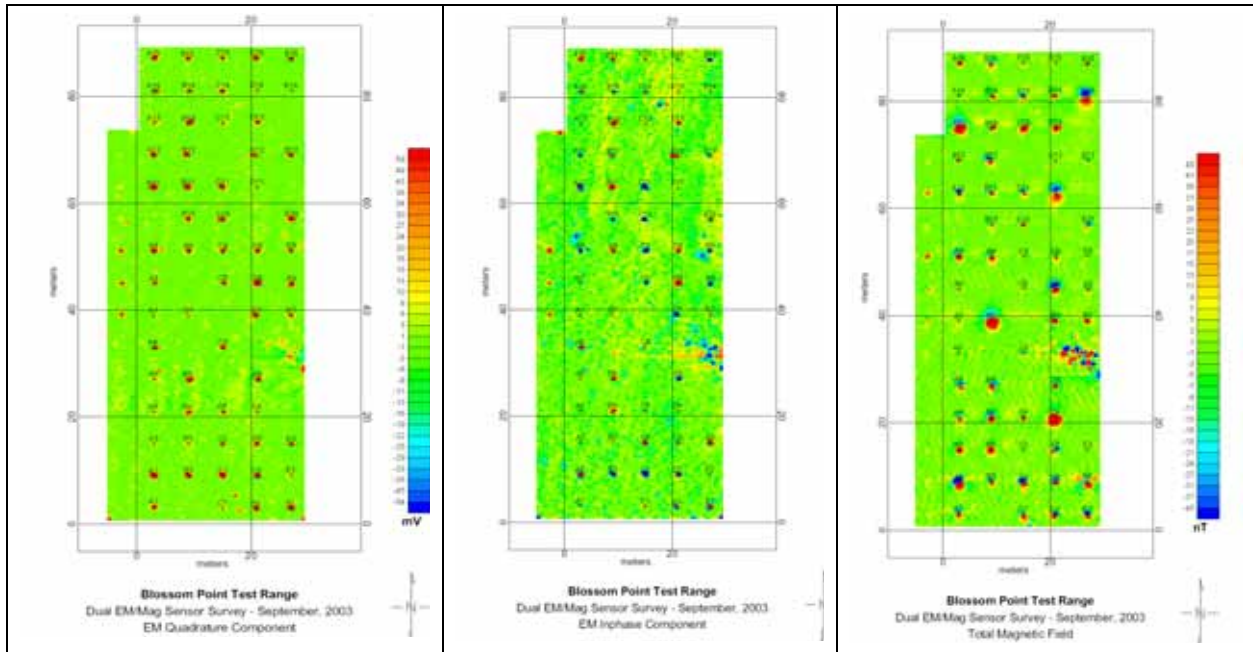
Figure 10. EM (Quadrature and Inphase) and Total Magnetic Field data collected in dynamic survey mode at the Blossom Point UXO test facility.

complementary nature of the two sensor technologies. For example target D-12 (second column from right, fourth row from top) is detected with both EM components but does not appear in the measured magnetic data. Conversely target D-11 (directly below D-12) only appears in the magnetometer data.

The S/N ratios (SNRs) for each target were calculated as:

$$SNR(dB) = 10 \times Log_{10} (\sum S^2/<n>^2),$$

where values for S are retrieved from a localized sample of data observed to be exhibiting an anomalous response over the target and values for n are retrieved from a similar (with respect to sample size) set of data collected over a non-anomalous area. Due to the structured nature of a magnetic total field dipolar response, the magnetic analytic signal was used for these calculations.

Using this definition of SNR, it was empirically determined that a threshold of 10 dB is required for reliable detection of the emplaced targets. Figure 11 shows the SNR results for the 61 emplaced targets at Blossom Point. The majority of targets (60 out of 61) exceed the SNR threshold for both the magnetic and EM data sets. This detection level is not unexpected

given the benign nature of the local geology and topography and relatively large caliber of the emplaced UXO. It is interesting to note that a number of targets would have been missed if only one of the data sets were collected. Figure 12 shows the percentage of targets detected by each data set as well as the aggregate.

Dual Sensor S/N for Emplaced Targets at the NRL Blossom Pt UXO Test Field
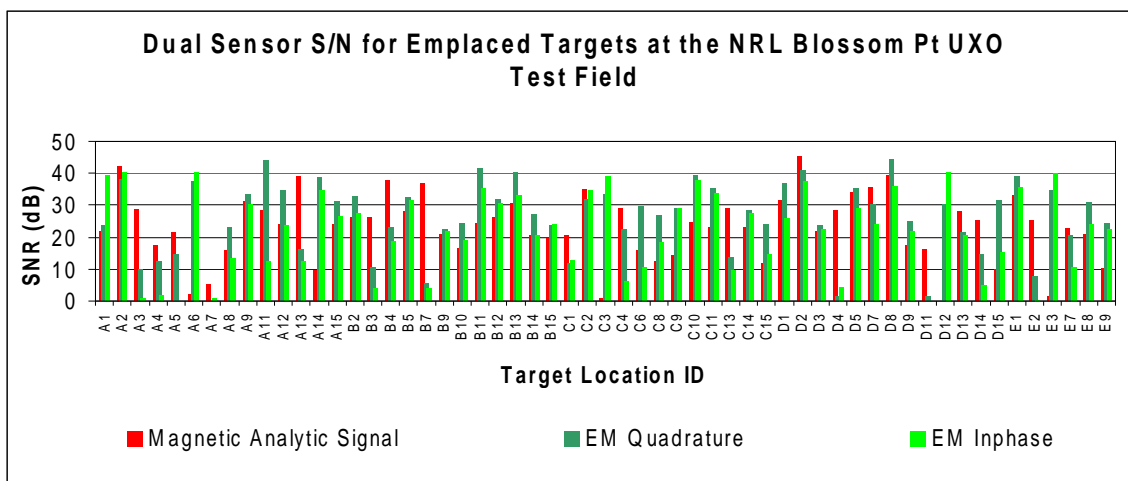
Figure 11. SNRs for dual sensor data collected at the Blossom Point UXO test field.

Dual Sensor Detection Performance at the Blossom Pt. Test Site
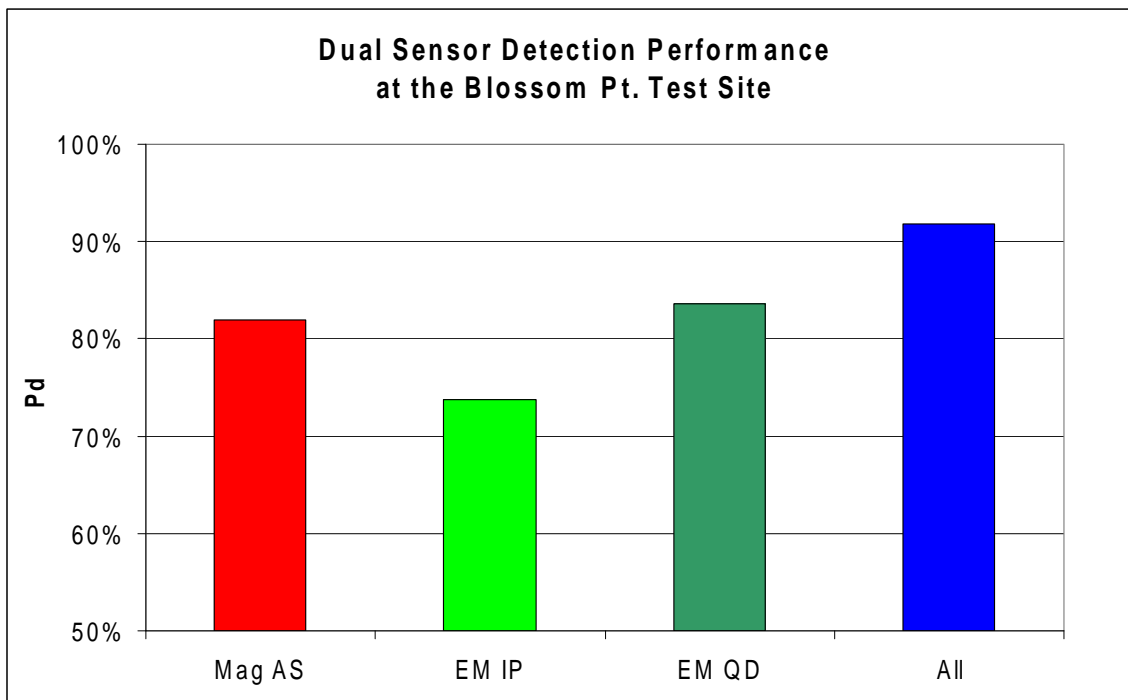
Figure 12. Percentage of total emplaced ordnance detected at the Blossom Point test field.

During the course of the survey a number of technical issues arose. The most serious of these was elevated noise levels in the magnetometer data (evident in the bottom third of the Total Magnetic Field map). After some investigation, it was found that one of the two wheel axles was magnetic (as luck would have it, only one axle was bench tested for this magnetism, and the problem was not found during that test). Fortunately, the NRL staff had a degaussing instrument on site, and the magnetic signature of the axle was reduced to insignificant levels. However, the subsequent sortie showed that the magnetometer noise was only slightly reduced. It was then assumed that the 0.5 m offset from the EM coil was not sufficient to reduce the EM heading errors. These noise levels are evident in the middle of the gridded image. After increasing the offset to 0.6 m, the noise was reduced to acceptable levels (i.e., less than that imposed by local geology). The top third of the grid was surveyed with these improvements. It bears mention that this problem is likely to arise in more rugged topography. In this case compensation of these heading errors is likely the best solution.

A second problem encountered was that the magnetometer would occasionally cease to record data. It was later determined that the data acquisition system would, under certain circumstances, send a character to the magnetometer counter board that effectively stopped proper operation of the magnetometer. Because the beta version of the data acquisition software did not provide a means to verify the magnetometer data (it only gave indication that the serial data was being received), this resulted in several sorties having to be repeated. This problem has since been resolved by disabling the data acquisition transmit line on the interconnecting cable. Future versions of the acquisition software will provide for viewing of the incoming magnetic data.

Subsequent to the dynamic survey, the data were analyzed using the dipole fit algorithms described above. The lack of accuracy of the data positioning prevents use of the results from these algorithms for anything other than deriving a coarse estimate of the target positions. Figure 13 shows the estimated target positions relative to the ground truth positions supplied by NRL. The spreading of these points in the East-West direction indicates that our Easting positions were less accurate than our Northing positions. This finding is consistent with expectations given the manner in which these data were positioned (North-South positioning is well constrained relative to the East-West positioning).
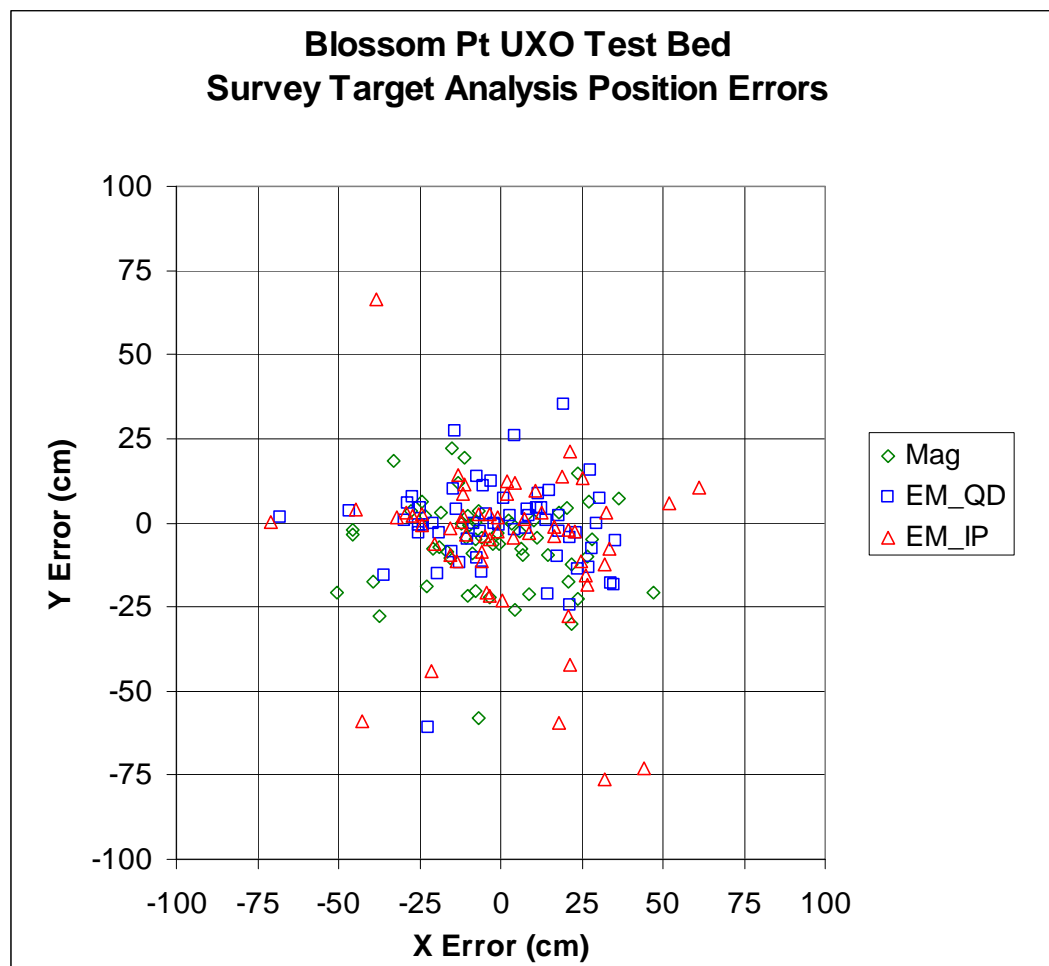
Figure 13. Errors in target positions derived from dynamic survey data at the Blossom Point UXO test facility.

Cued analysis tests

Because of the lack of accuracy in the positioning of the data during a detection survey (particularly when dead-reckoning is used), it was decided that a "cued analysis" of selected data targets would be performed after a given detection survey. During the Blossom Point trials, it was decided to test the cued analysis procedures on a series of ordnance placed in a test pit that was designed for this style of investigation. By doing so it was possible to test the cued analysis procedures as well as collect baseline EM73 data on a range of UXO at various depths and orientations.

Figure 14 shows the improved accuracy in the position estimates relative to those derived from the survey data (Figure 13). These results confirm that using a cued analysis approach to follow up on targets selected from a dynamic survey data set make it possible to position targets with a high degree of accuracy.
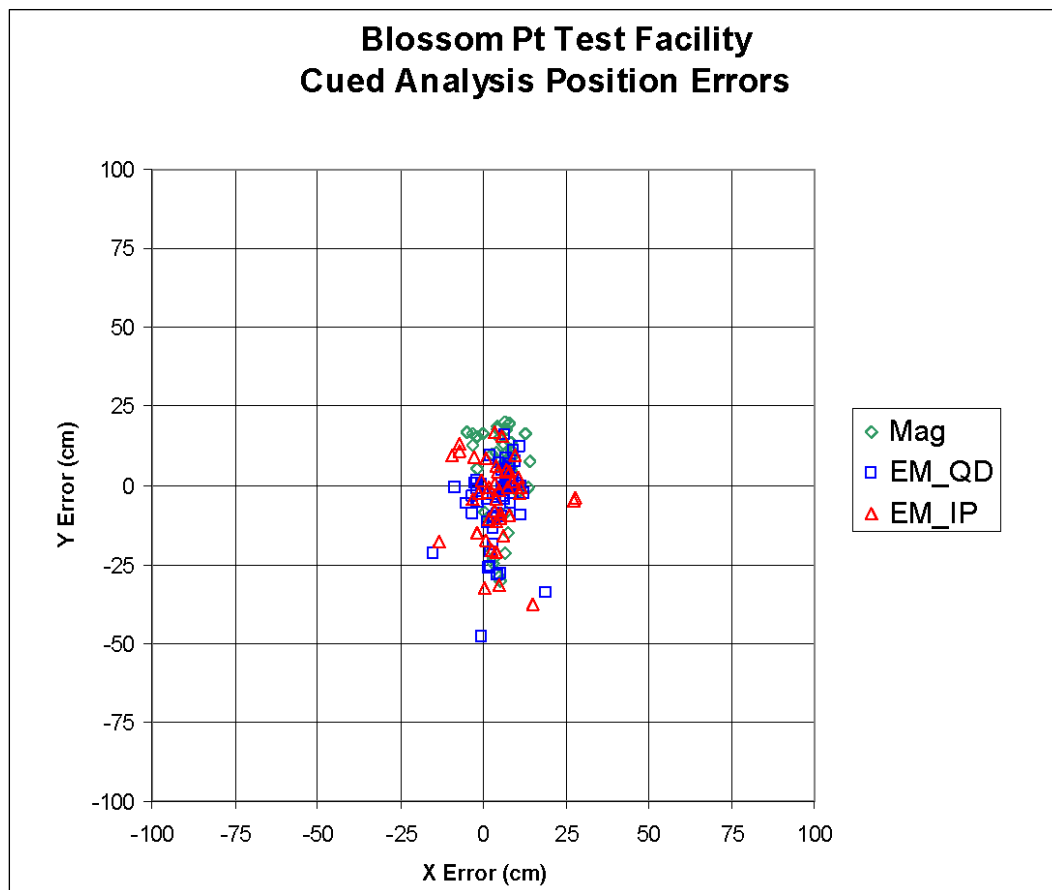
Figure 14. Errors in positions derived using cued analysis data collected at the Blossom Point UXO test facility.

Figure 15 presents the results of the EM analysis for selected targets. For each target the ratio of the primary beta to the average of the secondary betas provides an indication of aspect ratio, while the vertical error bars, representing each secondary beta, provide an indication of axial symmetry. It is of interest that the target groupings appear to spread with respect to magnitude of their responses. This result is primarily due to poor resolution of target depth in the analysis. This spreading may be mitigated by use of the magnetic data to constrain the target depth using joint or cooperative inversions (Pasion et al. 2002).
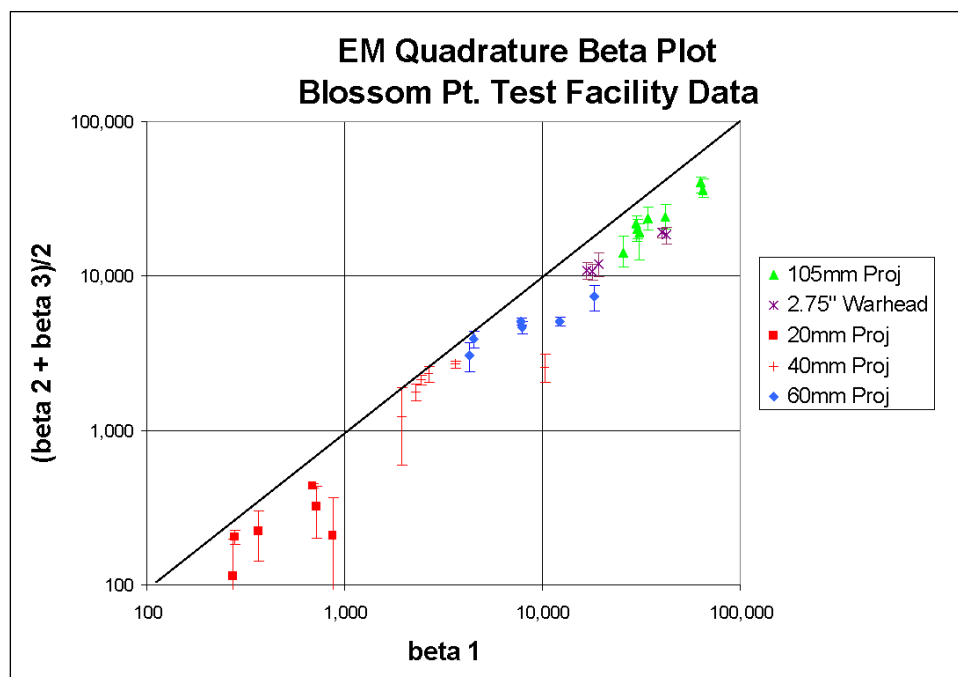
Figure 15. EM analysis results from data collected at the Blossom Point UXO test facility.

Field Test 2: Vicksburg, MS

The system was demonstrated at the ERDC UXO Test Site in Vicksburg, MS, during 7–9 October 2003. The purpose of this trial was to demonstrate to ERDC personnel the system deployment procedures and detection capabilities.

Site description

The ERDC UXO Test Site is located at the ERDC facilities in Vicksburg, MS. The field is a 30 m x 100 m rectangle that is relatively flat and devoid of vegetation other than grass. The local geophysical environment is benign with the exception of a large metal building situated approximately 30 m south of the survey area. The test field is seeded with small to medium size UXO and clutter targets. After correcting for the difference in the local reference system, the positioning errors were tabulated and are presented in Appendix A.

The site was surveyed as two separate blocks. The small UXO block was surveyed with a line spacing of 0.33 m and the western block was surveyed at 0.5-m spacing. All survey lines were traversed in an East-West direction, parallel to the building adjacent to the test field area. By doing so, any

magnetic signal from the building was removed through the use of simple de-median filters. The survey data were positioned using the same dead reckoning techniques as used for the Blossom Point shakedown testing.

Survey results

The survey data for the small UXO block are presented in Figure 16. The top two panels of this figure are the magnetic data; Total Magnetic Field and Analytic Signal. The bottom two panels are the Quadrature and Inphase components of the EM response. Targets 10 through 37 are the emplaced UXO and clutter items. Targets 15, 16, and 17 were clutter items that were not detected by either technology, which is most likely due to the fact that they were nonmagnetic and too small and deep for the EM to detect. Figure 17 shows the SNR for each of the emplaced targets.

Based upon the dynamic survey results, the locations of selected targets were flagged for follow up cued analysis investigations. The primary purpose of the cued investigations was to provide accurate position estimates of the targets. To achieve this goal, positions for each flag were surveyed by ERDC personnel. A 5 x 9 point grid spaced at 0.25-m intervals was marked around each flag. Data collected at each of these intervals were analyzed using the dipole fit algorithms described above. Figure 18 presents the data collected over each target.

Because of the high degree of accuracy in the positioning of the cued data relative to the flag positions, it was possible to estimate the target position relative to the flag with a high degree of confidence for many of the targets. Knowing the position of the flags in WGS84 UTM (Universal Transverse Mercator) coordinates allowed for transform of the target position estimates to this projection/coordinate system. Table 1 shows the position estimates for each target. The positions of the emplaced targets that went undetected were estimated by applying an offset equal to the mean UTM to local ground truth offset of the detected targets. The coarse confidence level reported in Table 1 is based upon the target signal levels, presence of overlapping signal in the analyzed data, and the dipole fit coherence.
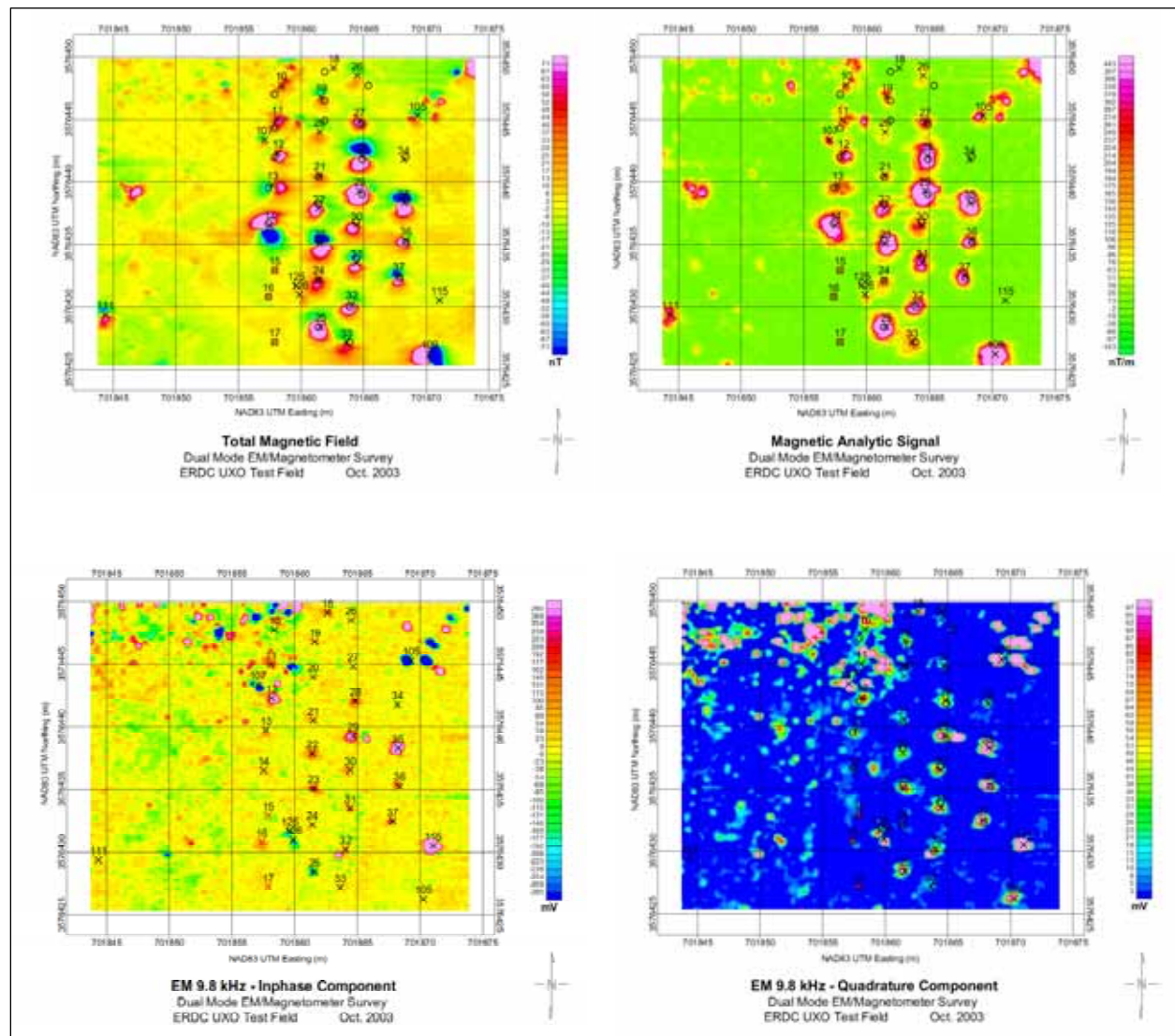
Figure 16. Survey data collected over the ERDC UXO test field using dynamic data acquisition.
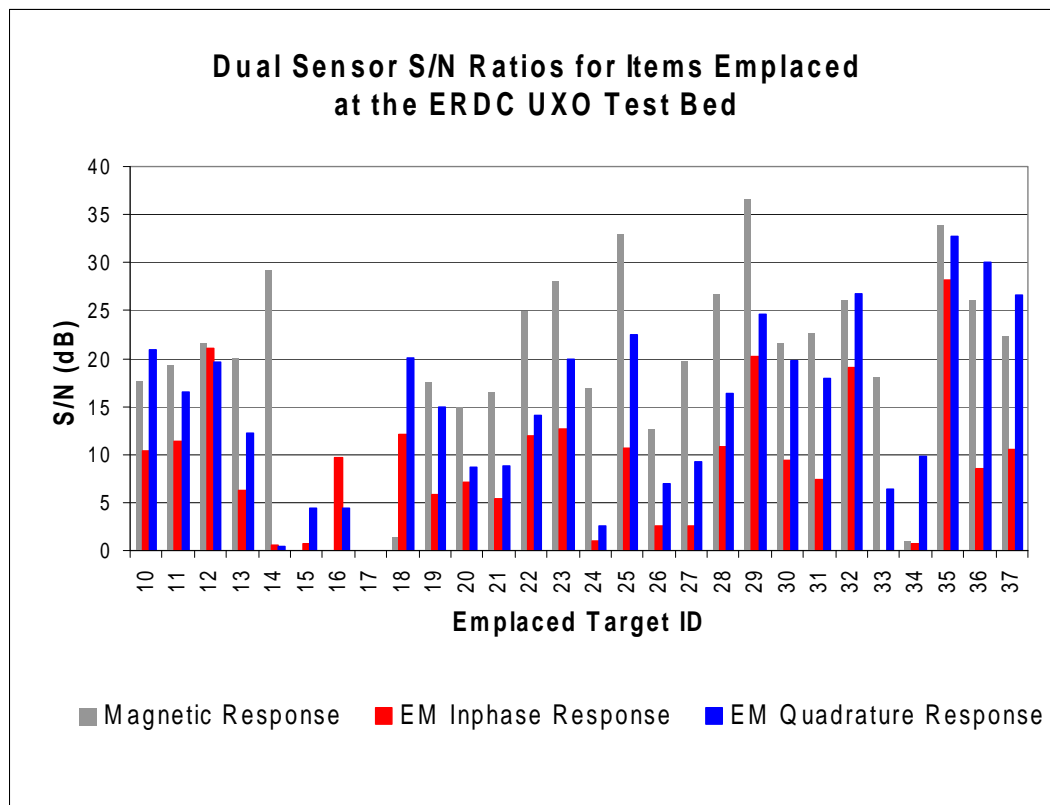
Figure 17. SNRs for the magnetic and EM data collected during a dynamic survey of the ERDC UXO test field.
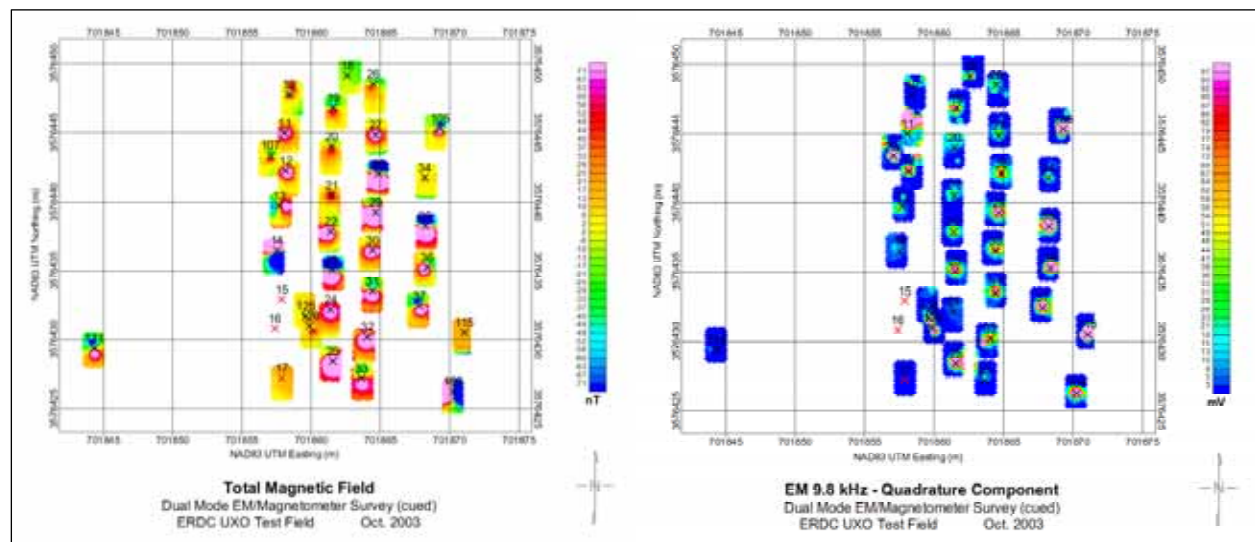

Figure 18. Data collected over selected targets at the ERDC UXO test field using a cued analysis approach.

Table 1. Position estimates for each target.

ID	Flag Positions				Mag					EM Quad					Final Positions			
	Easting	Northing	Loc_X	Loc_Y	Xoff	Yoff	Depth	Coh.	S/N	Xoff	Yoff	Depth	Coh.	S/N	Easting	Northing	Position Conf.	
1															701781.87	3576444.73		not analyzed
2															701786.37	3576429.23		not analyzed
3															701792.87	3576437.23		not analyzed
4	701796.32	3576444.07	17.2	24.8	0.24	0.25	1.2	0.994	15	0.08	0.14	0.67	0.665	-	701796.56	3576444.31	medium	no em
5															701800.87	3576428.23		not analyzed
6	701803.16	3576443.85	24.0	24.4	-0.07	-0.11	1.1	0.996	25	-0.43	0.10	0.47	0.95	-	701803.09	3576443.74	medium	no em
7															701818.37	3576438.73		not analyzed
8															701819.87	3576428.23		not analyzed
9	701829.01	3576429.42	50.1	9.7	0.92	0.00	2.4	0.928	10	3.40	0.74	1.1	0.766	-	701829.93	3576429.42	low	no em
10	701858.61	3576447.54	79.7	28.2	-0.22	0.21	0.1	0.636	18	-0.03	-0.09	1.14	0.698	21	701858.40	3576447.75	low	High clutter area
11	701858.44	3576444.99	79.5	25.5	-0.35	-0.02	0.9	0.973	19	-0.20	0.91	0.23	0.887	17	701858.09	3576444.97	high	High clutter area
12	701858.41	3576441.92	79.5	22.6	-0.25	0.37	0.6	0.983	22	0.03	0.93	0.81	0.715	20	701858.16	3576442.29	high	some clutter
13	701857.76	3576439.54	78.8	20.1	-0.05	0.23	0.8	0.988	20	-0.13	0.12	0.52	0.805	12	701857.71	3576439.76	medium	
14	701857.34	3576436.19	78.2	16.9	0.17	0.34	0.8	0.999	29	-0.05	0.44	0.3	0.836	0	701857.52	3576436.52	high	
15															701857.87	3576432.93		not analyzed (low signal for EM and Mag)
16															701857.37	3576430.83		not analyzed (low signal for EM and Mag)
17	701857.92	3576426.98	79.0	7.5			5.3	0.867	(5)			0.85	0	-	701857.87	3576427.23		low S/N for Mag and EM
18	701862.80	3576449.19	83.9	29.8	0.56	0.70	3.1	0.908	1	-0.19	-0.08	0.23	0.933	20	701862.61	3576449.11	medium	non-ferrous
19	701861.83	3576446.57	82.9	27.2	-0.23	0.23	0.5	0.991	18	-0.54	0.23	0.41	0.946	15	701861.60	3576446.80	high	
20	701861.45	3576443.42	82.5	24.4	0.04	0.56	0.7	0.972	15	-0.37	2.15	0.4	0.641	9	701861.48	3576443.98	medium	
21	701861.31	3576440.10	82.4	20.8	0.16	0.42	0.7	0.97	16	0.16	0.12	1.19	0.777	9	701861.48	3576440.52	high	
22	701861.32	3576437.77	82.4	18.3	0.09	0.11	0.8	0.995	25	0.10	-0.05	0.75	0.987	14	701861.41	3576437.88	high	
23	701861.57	3576435.03	82.7	15.5	-0.07	0.05	0.6	0.996	28	-0.01	0.11	0.45	0.996	20	701861.51	3576435.08	high	
24	701861.32	3576431.61	82.4	12.3	0.09	0.56	1.3	0.996	17	0.59	0.46	1.04	0	2	701861.40	3576432.17	high	

ID	Flag Positions				Mag					EM Quad					Final Positions			
	Easting	Northing	Loc_X	Loc_Y	Xoff	Yoff	Depth	Coh.	S/N	Xoff	Yoff	Depth	Coh.	S/N	Easting	Northing	Position Conf.	
25	701861.39	3576428.37	82.5	9.0	0.17	0.05	0.7	0.981	33	0.21	0.20	0.45	0.997	23	701861.56	3576428.42	high	
26	701864.59	3576447.75	85.6	29.0	-0.09	0.77	0.6	0.911	13	-0.23	0.66	0.2	0.85	7	701864.49	3576448.51	high	
27	701864.67	3576444.91	85.7	25.5	-0.02	-0.08	0.7	0.987	20	-0.07	0.16	0.5	0.955	9	701864.65	3576444.83	high	
28	701864.83	3576441.86	85.9	22.6	0.02	0.20	0.8	0.994	27	0.10	0.27	0.64	0.988	16	701864.85	3576442.06	high	
29	701864.45	3576439.17	85.5	19.7	0.20	0.09	0.7	0.995	37	0.17	0.12	0.55	0.998	25	701864.65	3576439.26	high	
30	701864.18	3576436.38	85.3	17.0	0.25	0.16	0.8	0.983	22	0.42	0.19	0.68	0.995	20	701864.43	3576436.54	high	
31	701864.43	3576433.41	85.5	14.0	0.01	0.09	0.7	0.977	23	0.15	0.11	0.72	0.993	18	701864.43	3576433.50	high	
32	701863.83	3576429.68	84.9	10.5	0.23	0.53	0.7	0.989	26	-0.02	0.27	0.31	0.944	27	701864.06	3576430.21	medium	second target close by (.5m SW)
33	701863.71	3576427.02	84.8	7.7	-0.07	0.17	1.2	0.985	18	-0.05	0.46	0.41	0.852	6	701863.64	3576427.19	high	
34	701868.33	3576441.69	89.4	22.3	-0.39	0.06	1.0	0.661	1	-0.12	0.09	0.52	0.971	10	701868.21	3576441.78	high	low ferrous content/ shallow
35	701868.30	3576437.99	89.4	18.7	-0.05	0.32	0.5	0.993	34	-0.03	0.32	0.34	0.999	33	701868.25	3576438.31	high	
36	701868.20	3576435.30	89.3	15.8	0.18	-0.02	0.5	0.977	26	0.23	-0.03	0.38	0.999	30	701868.38	3576435.28	high	
37	701867.73	3576432.32	88.8	12.9	0.10	0.13	0.5	0.99	22	0.08	0.17	0.34	0.998	27	701867.82	3576432.45	high	
105	701869.02	3576445.17	90.1	25.9	0.28	0.15	0.3	0.984	14	0.27	0.13	0.29	0.999	23	701869.30	3576445.31	high	
107	701856.96	3576443.28	78.1	23.9	0.16	0.06	0.2	0.855	14	0.11	0.08	0.17	0.997	19	701857.07	3576443.36	high	
109	701870.20	3576425.95	91.3	6.7	0.06	0.31	0.5	0.989	26	0.05	0.32	0.45	0.997	24	701870.26	3576426.26	high	
111	701844.33	3576429.36	65.4	10.0	0.00	0.01	0.7	0.969	13	-0.52	0.21	0.56	0.513	(1)	701844.34	3576429.38	medium	
115	701870.99	3576430.41	92.1	11.2					(0)	0.07	0.11	0.2	0.993	38	701871.05	3576430.52	high	non-ferrous
125	701859.50	3576432.31	80.6	12.2	0.30	-1.00	0.3	0.408	9	0.11	-0.62	0.31	0.985	21	701859.61	3576431.69	high	small shallow target
126	701859.97	3576430.77	81.1	11.2	1.85	-0.47	1.1	0.294	20	-0.09	0.22	0.44	0.885	32	701859.88	3576430.99	high	small shallow target

6   Conclusions and Recommendations

Conclusions are as follows:

1. Magnetic and EM sensor technologies can be fielded simultaneously on a man-portable platform provided the EM field is oscillating >> 200 Hz and the bias imposed by the EM field on the measured magnetic data is properly mitigated.
2. The EM-induced bias was minimized for dynamic survey applications by separating the magnetometer from the EM transmitter coils by 0.6 m. This separation was unnecessary for static data collection as the bias was manifested as an easily corrected offset in the magnetic data.
3. Bench testing of the system showed that the utility of each sensor (with respect to detection and characterization of UXO-like targets) was maintained during their simultaneous deployment. Dipole fit algorithms applied to both the magnetic and electromagnetic data provided reasonable target feature estimates.
4. The EM-induced bias in the magnetic data was mitigated during these tests by physically offsetting the magnetometer from the EM transmitter coils. In both detection surveys, the aggregate detection rate exceeded the detection rates for the individual component sensor technologies, demonstrating the complementary nature of the technologies.
5. Cued analysis tests performed on Blossom Point data showed that features can be estimated using physics-based analyses. In particular, the location estimate errors provided by these analyses were consistently less than 0.3 m. Cued analysis data collected at the ERDC test site were verified with ground truth data and were correctly positioned within 0.43 m. When the largest outlier was removed, the error was less than 0.36 m.

Recommendations are as follows:

1. Redesign the man-portable dual-sensor system as a handheld system.
2. Reconfigure the EM sensor head to lower the overall weight and improve the balance of the system.
3. Implement magnetic compensation to remove the EM bias, which will allow greater flexibility with respect to the physical location of the magnetometer relative to the EM coils.
4. Include a multi-frequency transmitter to the sensor to provide improved EM-based detection and characterization capabilities.

References

Bell, T., and B. Barrow. 2000. Subsurface discrimination using handheld electromagnetic induction sensors. International Geoscience and Remote Sensing Symposium (IGARSS 2000). Honolulu, HI, 24–28 July 2000.

Khadr, N, B. Barrow, T. H. Bell, and H. Nelson. 1998. Target shape classification using electromagnetic induction sensor data. UXO Forum 1998, Anaheim, CA, 5–7 May 1998.

Nelson, H., T. Alshuler, E. Rosen, J. McDonald, B. Barrow, and N. Khadr. 1998a. Magnetic modeling of UXO and UXO-like targets and comparison with signatures measured by MTADS. UXO Forum 1998. Anaheim, CA, 5–7 May 1998.

Nelson, H., J. McDonald, and R. Robertson. 1998b. Design and construction of the NRL baseline ordnance classification test site at Blossom Pt. Naval Research Laboratory. NRL/MR/6110-00-8437, March 20, 1998.

Pasion, L., S. Billings, and D. Oldenburg. 2003. Joint and cooperative inversion of magnetics and time domain electromagnetic data for the characterization of UXO, 15th Annual Symposium on the Application of Geophysics to Engineering and Environmental Problems (SAGEEP 2003), San Antonio, TX, 6–10 April 2002.

Appendix A: Differences in AETC Anomaly Data and Ground Truth

Table A1 shows the difference between the AETC final position for each anomaly and the corrected ground truth for the ERDC UXO test site. From the difference data in Table A1, the average positioning error of 0.198 m for the northing and 0.379 m for the easting was calculated. Also, from the difference data in Table A1, the standard deviation for the northing and the easting was determined to be 0.168 m and 0.675 m, respectively.

Table A1. Differences in northing and easting between AETC data and ground truth.

Item Number	Northing (m)	Easting (m)
1	0.168	0.132
2	0.168	0.132
3	0.168	0.132
4	0.048	0.178
5	0.168	0.132
6	0.822	0.048
7	0.168	0.132
8	0.822	0.132
9	0.168	0.192
10	0.168	0.662
11	0.142	0.352
12	0.374	0.422
13	0.294	0.472
14	0.086	0.282
15	0.168	0.132
16	NA*	NA
17	0.168	3.868
18	0.066	0.872
19	0.076	0.362
20	0.782	0.242
21	0.256	0.242
22	0.182	0.172
23	0.082	0.272
24	0.208	0.162
25	0.158	0.322
26	0.434	0.748
27	0.146	0.088
28	0.116	0.112
29	0.116	0.088
30	0.122	0.192

Item Number	Northing (m)	Easting (m)
31	0.262	0.192
32	0.166	0.322
33	0.128	0.098
34	0.082	0.028
35	0.052	0.012
36	0.218	0.0142
37	0.226	0.082
105	NA	NA
107	NA	NA
109	NA	NA
111	NA	NA
115	NA	NA
126	NA	NA
126	0.186	1.858

* NA means no target was located at or near the
AETC data position.

Figure A1 shows the positions of the AETC selections after the difference of the local reference system was removed.
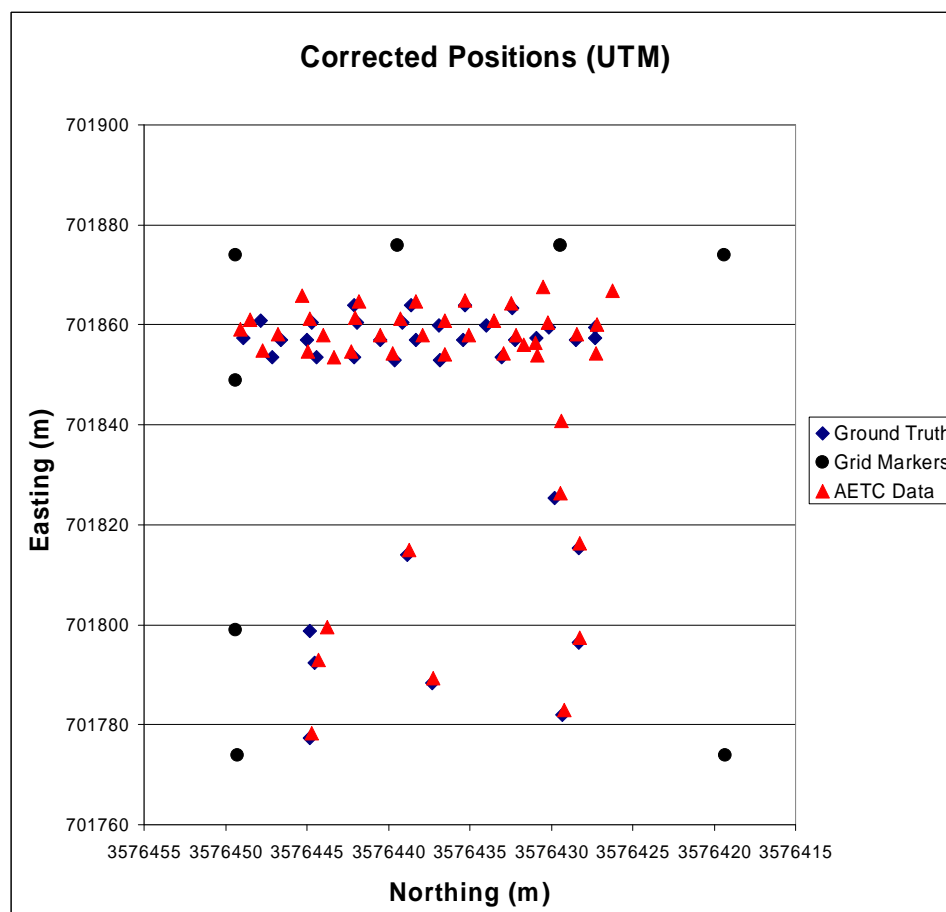

Figure A1. Positions of AETC selections and ground truth.

REPORT DOCUMENTATION PAGE

Public reporting burden for this collection of information is estimated to average 1 hour per response, including the time for reviewing instructions, searching existing data sources, gathering and maintaining the data needed, and completing and reviewing this collection of information. Send comments regarding this burden estimate or any other aspect of this collection of information, including suggestions for reducing this burden to Department of Defense, Washington Headquarters Services, Directorate for Information Operations and Reports (0704-0188), 1215 Jefferson Davis Highway, Suite 1204, Arlington, VA 22202-4302. Respondents should be aware that notwithstanding any other provision of law, no person shall be subject to any penalty for failing to comply with a collection of information if it does not display a currently valid OMB control number. **PLEASE DO NOT RETURN YOUR FORM TO THE ABOVE ADDRESS.**

1. REPORT DATE *(DD-MM-YYYY)* February 2008	2. REPORT TYPE Final report	3. DATES COVERED *(From - To)*

4. TITLE AND SUBTITLE Multi-Sensor Systems Development for UXO Detection and Discrimination: Man-Portable Dual Magnetic/Electromagnetic Induction Sensor	5a. CONTRACT NUMBER
	5b. GRANT NUMBER
	5c. PROGRAM ELEMENT NUMBER
6. AUTHOR(S) David Wright, Hollis H. Bennett, Jr., Linda Peyman Dove, John H. Ballard, Morris P. Fields, Tere A. Demoss, and Dwain K. Butler	5d. PROJECT NUMBER
	5e. TASK NUMBER
	5f. WORK UNIT NUMBER

7. PERFORMING ORGANIZATION NAME(S) AND ADDRESS(ES) See reverse.	8. PERFORMING ORGANIZATION REPORT NUMBER ERDC/EL TR-08-9

9. SPONSORING / MONITORING AGENCY NAME(S) AND ADDRESS(ES) U.S. Army Corps of Engineers Washington, DC 20314-1000	10. SPONSOR/MONITOR'S ACRONYM(S)
	11. SPONSOR/MONITOR'S REPORT NUMBER(S)

12. DISTRIBUTION / AVAILABILITY STATEMENT

Approved for public release; distribution is unlimited.

13. SUPPLEMENTARY NOTES

14. ABSTRACT

An unexploded ordnance (UXO) survey instrument that simultaneously collects total field magnetic data and frequency domain electromagnetic (FDEM) data was developed and tested for the detection and characterization of buried UXO objects. The system comprised an FDEM sensor operating at a single frequency of 9.8 kHz and a cesium vapor magnetometer. The system was tested in dynamic survey (detection) and cued analysis (characterization) modes at the Naval Research Laboratory Blossom Point UXO test facility in Maryland and the U.S. Army Engineer Research and Development Center (ERDC) UXO test site in Mississippi.

During these tests, electromagnetic (EM)-induced bias in the magnetic data was mitigated by physically offsetting the magnetometer from the EM transmitter coils. In both detection surveys, the aggregate detection rate exceeded the detection rates for the individual component sensor technologies. The cued analysis tests performed at Blossom Point showed that features can be estimated using physics-based analyses. The location estimate errors provided by these analyses were consistently less than 0.3 m. The cued analysis data collected at the ERDC UXO test site have been used to provide position estimates for most of the emplaced targets at this site.

15. SUBJECT TERMS

See reverse.

16. SECURITY CLASSIFICATION OF:			17. LIMITATION OF ABSTRACT	18. NUMBER OF PAGES	19a. NAME OF RESPONSIBLE PERSON
a. REPORT UNCLASSIFIED	b. ABSTRACT UNCLASSIFIED	c. THIS PAGE UNCLASSIFIED		40	19b. TELEPHONE NUMBER *(include area code)*

7. PERFORMING ORGANIZATION NAME(S) AND ADDRESS(ES)

AETC Incorporated
120 Quade Drive, Cary, NC 27513-7400;
U.S. Army Engineer Research and Development Center
Environmental Laboratory
3909 Halls Ferry Road, Vicksburg, MS 39180-6199;
Alion Science and Technology Corporation
U.S. Army Engineer Research and Development Center
3909 Halls Ferry Road, Vicksburg, MS 39180-6199

15. (Continued)

AETC Incorporated
Dual magnetic/EMI sensor
Electromagnetic induction (EMI)
EM73
Frequency domain electromagnetic (FDEM)
G823A cesium vapor magnetometer
Total field magnetic
TFM
Unexploded ordnance (UXO)
UXO test site